

# Raman cooling and heating of two trapped Ba<sup>+</sup> ions

D. Reiß, K. Abich, W. Neuhauser, Ch. Wunderlich, P.E. Toschek  
*Institut für Laser-Physik, Universität Hamburg, Jungiusstr. 9, 20355 Hamburg, Germany*  
(October 24, 2018)

We study cooling of the collective vibrational motion of two <sup>138</sup>Ba<sup>+</sup> ions confined in an electrodynamic trap and irradiated by laser light close to the resonances S<sub>1/2</sub>-P<sub>1/2</sub> (493 nm) and P<sub>1/2</sub>-D<sub>3/2</sub> (650 nm). The motional state of the ions is monitored by a spatially resolving photomultiplier. Depending on detuning and intensity of the cooling lasers, macroscopically different motional states corresponding to different ion temperatures are observed. We also derive the ions' temperature from detailed analytical calculations of laser cooling taking into account the Zeeman structure of the energy levels involved. The observed motional states perfectly match the calculated temperatures. Significant heating is observed in the vicinity of the dark resonances of the Zeeman-split S<sub>1/2</sub>-D<sub>3/2</sub> Raman transitions. Here two-photon processes dominate the interaction between lasers and ions. Parameter regimes of laser light are identified that imply most efficient laser cooling.

32.80.Pj, 42.50.Vk, 03.67.Lx

## I. INTRODUCTION

In order to implement conditional quantum dynamics of qubits represented by the internal structure of individual ions in a Paul trap, a vibrational mode of the entire ion string is used. Cirac and Zoller [1] have suggested a method for conditional dynamics that requires the ions to be cooled to their vibrational ground state. Here, the vibrational state represents a “bus” qubit that gets entangled with the ions' internal states by stimulated transitions, where the absorption (or emission) of a photon is coupled with the emission (or absorption) of a vibrational quantum.

The recently proposed Sørensen-Mølmer scheme [2] incorporates two-photon transitions in order to directly entangle the internal states of the ions. Here, the vibrational mode is only virtually excited. In this way the contribution of higher vibrational excitations can be made to destructively interfere. In this way, the scheme does not require cooling to the vibrational ground state, but admits population in higher vibrational levels.

In general, the manipulation of the motion of trapped particles by light relies on the coupling of electronic and motional degrees of freedom via the scattering of photons. Here, the important figure of merit is the Lamb-Dicke parameter (LDP)  $\eta$ , its square given by the ratio of the recoil energy transferred when scattering a photon, and the energy of the vibrational quantum [3]. For small  $\eta$ , transition processes involving the creation or annihilation of  $n$  vibrational quanta (i.e.  $n$ th order sideband transitions) are suppressed by the factor  $\eta^{2n}$ . Therefore, a small LDP allows only linear coupling (involving only single-phonon transitions) between electronic and vibrational degrees of freedom. This Jaynes-Cummings type of coupling [4] is prerequisite for many schemes suggested in quantum information processing including the mentioned implementations [1,2].

Plenio and Knight [5] have proposed to drive the interaction between electronic and vibrational degrees of

freedom by tuning *strong* laser light to the resonance frequency, instead of the sideband. In this case, the light intensity imposes a specific light shift on the ions that selects the desired transition. By doing so, the time needed for conditional dynamics is reduced, as compared with the Cirac-Zoller scheme, thus reducing the effect of decoherence. Here, too, the LDP plays a crucial role as the fidelity of such a fast quantum gate is  $f \approx 1 - \frac{1}{2}\eta^2$ .

While the Sørensen-Mølmer scheme does not require ground-state cooling, it still demands low vibrational quantum numbers (i.e.  $\eta^2(n+1) \ll 1$ ). Thus, laser cooling is essential for quantum information processing in ion traps, and it is desirable to have at hand robust cooling techniques that are suited for reaching low vibrational excitation at moderate technological expenditure on the side of the laser sources. In particular, cooling of the collective motion of several particles is prerequisite for implementing conditional quantum dynamics with trapped ions.

It has been known for some time that the motion of trapped particles strongly depends on laser cooling. With a single trapped particle, distinct macroscopic motional states have been observed with different parameters of the cooling lasers [6]. With a cloud of ions, changes in the temperature induced by laser cooling cause phase transitions between a crystalline and an evaporated state [7,8]. These macroscopically distinct states indicate the specific temperature achieved by laser cooling.

In this paper we investigate the macroscopic motional states of two trapped <sup>138</sup>Ba<sup>+</sup> under the action of laser cooling. In Sec. II, the theory of laser cooling of the collective motion of two charged particles trapped in an anisotropic harmonic potential is outlined. If the particles obey the Lamb-Dicke limit, the cooling rate and the achievable temperature are calculable without any free parameter. We fully take into account the multi-level structure of the involved ions, thus allowing for any type of cooling process, such as Doppler [9], sideband [10] and Raman cooling [11]. In Sec. III we describe the ex-

perimental setup and present the results of the measurements. Phase transitions between macroscopically distinct states are observed. The parameter values at which these transitions take place perfectly agree with the values calculated from the theoretical model. In Sec. IV we use the model to find optimized laser parameters for cooling the collective motion of the ions.

## II. THEORY

### A. Collective Motion

We consider the collective motion of two ions of mass  $m$  in a three-dimensional (3D) harmonic trapping potential

$$V_{\text{trap}}(\mathbf{r}_j) = \frac{m}{2} (\omega_x^2 x_j^2 + \omega_y^2 y_j^2 + \omega_z^2 z_j^2), \quad (1)$$

which is the same for both ions ( $j = 1, 2$ ). Since each of the ions carries one positive elementary charge  $e$ , they repel each other by the Coulomb interaction

$$V_C(\mathbf{r}_1, \mathbf{r}_2) = \frac{e^2}{4\pi\epsilon_0 |\mathbf{r}_1 - \mathbf{r}_2|}. \quad (2)$$

The potential is simplified by using center-of-mass and relative coordinates

$$\mathbf{R} \equiv \frac{\mathbf{r}_1 + \mathbf{r}_2}{2} \quad \text{and} \quad \mathbf{r} \equiv \mathbf{r}_2 - \mathbf{r}_1. \quad (3)$$

With the definition of total and reduced masses  $M = 2m$  and  $\mu = m/2$ , one gets

$$V(\mathbf{R}) = \frac{M}{2} (\omega_x^2 X^2 + \omega_y^2 Y^2 + \omega_z^2 Z^2) \quad (4)$$

for the center-of-mass motion, corresponding to the motion of a single trapped particle with the original oscillation frequencies, but twice the ions mass.

The potential for the relative motion is

$$V(\mathbf{r}) = \frac{\mu}{2} (\omega_x^2 x^2 + \omega_y^2 y^2 + \omega_z^2 z^2) + \frac{e^2}{4\pi\epsilon_0 |\mathbf{r}|}. \quad (5)$$

If the trap frequencies slightly differ (as they do in our experiment, see Table I) this potential does not show spherical symmetry. With  $\omega_x < \omega_y < \omega_z$  holding, the potential has absolute minima on the  $x$  axis and saddle points on the  $y$  and  $z$  axis at

$$\mathbf{r}_{0,q} = \pm \sqrt[3]{\frac{e^2}{4\pi\epsilon_0 \mu \omega_q^2}} \mathbf{e}_q, \quad q = x, y, z. \quad (6)$$

Figure 1 shows the potential in the  $(x, y)$  plane. It is clear that for high enough temperature, i.e. at a mean motional energy  $E_{\text{ex}}$  comparable with the potential barrier at the saddle point on the  $y$ -axis

$$\Delta V_y = \frac{3}{2} \sqrt[3]{\left(\frac{e^2}{4\pi\epsilon_0}\right)^2 \mu (\omega_y^{2/3} - \omega_x^{2/3})}, \quad (7)$$

the ions can move freely in a ring-shaped region in the  $(x, y)$  plane. However, at low temperature, the relative motion is restricted to the wells, i.e., the ions will appear at approximately fixed positions. The same argument can be applied to the  $z$ -direction: For even higher energies  $E_{\text{ex}} \gtrsim \Delta V_z$  the motional state changes from a ring to a sphere. All three motional states have been observed in our experiment. However, in the following we shall focus on the transition between the localized and the ring state, as we are mainly interested in laser cooling in the low-temperature regime.

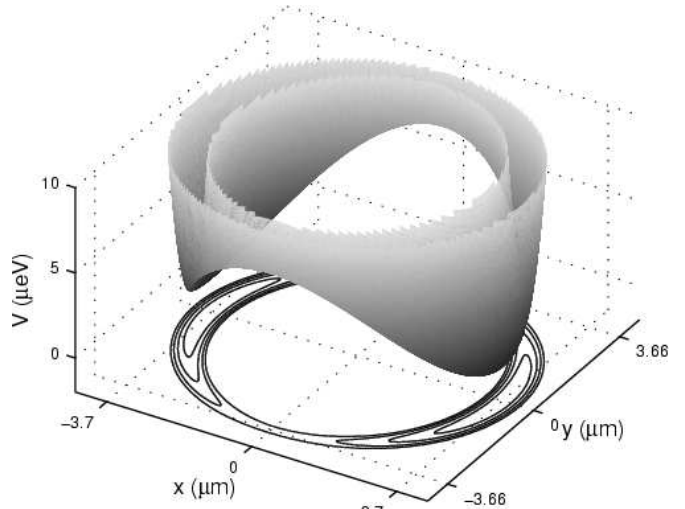


FIG. 1. Effective double well potential  $V(x, y)$  for the relative motion of two trapped  $^{138}\text{Ba}^+$  ions (trap frequencies as given in Table I). The contour lines correspond to  $V = 2, 4, 6, 8 \mu\text{eV}$ .

In the localized state the potential can be approximated around the minimum at  $\mathbf{r}_{0,x}$ . Expanding up to second order in the displacement  $\tilde{\mathbf{r}} \equiv \mathbf{r} - \mathbf{r}_{0,x}$  one gets

$$V(\mathbf{r}) = V(\mathbf{r}_{0,x}) + \frac{\mu}{2} (\tilde{\omega}_x^2 \tilde{x}^2 + \tilde{\omega}_y^2 \tilde{y}^2 + \tilde{\omega}_z^2 \tilde{z}^2) \quad (8)$$

with local frequencies

$$\tilde{\omega}_x = \sqrt{3}\omega_x, \quad \tilde{\omega}_{y,z} = \sqrt{\omega_{y,z}^2 - \omega_x^2} \quad (9)$$

(c.f. Table I)

Mode	$X$	$Y$	$Z$	$\tilde{x}$	$\tilde{y}$	$\tilde{z}$
$\omega/2\pi\text{MHz}$	1.0035	1.0220	1.0530	1.7381	0.1936	0.3191
$\eta_{493}$	0.044	0.044	0.043	0.034	0.101	0.079
$\eta_{650}$	0.034	0.033	0.033	0.026	0.077	0.060
$\eta_{1762}$	0.012	0.012	0.012	0.009	0.028	0.022

TABLE I. Frequencies and Lamb-Dicke parameters for the different vibrational modes. Note that the geometrical factor  $(\mathbf{k}_l \cdot \mathbf{e}_q)$  is included in the LDPs (Eq. 15). In the present experiment the angle of incidence is  $45^\circ$  to all directions, yielding a factor of  $1/\sqrt{3}$ .

## B. Laser Cooling of the collective motion

The mechanical effect of irradiating ions with laser light leads to thermalization of the motional degrees of freedom. The corresponding cooling rate and steady-state temperature depend on the electronic level scheme and laser parameters; they are calculated in this section. The key to the theory presented here is the well-known Lamb-Dicke limit: As long as the ions are localized near the minima of the potential, their spatial extension is much smaller than the wavelength of the exciting laser light. In this case, the photon recoil operator  $e^{i\mathbf{k}_l \cdot \mathbf{r}}$ , i.e. the coupling of the the internal dynamics to the ions motion, can be expanded in the LDP. Since the LDP is small, dynamics due to this coupling is slow compared with the internal dynamics that may be adiabatically eliminated. This reduction leads to a master equation for the motional degrees of freedom, where the involved transition rates depend on steady-state expectation values of internal operators. This procedure and its application to a single  $\text{Ba}^+$  ion has been described in [12].

We do not account for dipole-dipole interaction between the two ions, since the separation of the two ions is large as compared to the optical wavelengths used ( $r_0/\lambda \approx 8$ .) Even though processes caused by this interaction possibly could be observed [13], they are rare, compared with the single-ion scattering, and their influence on the collective motion is negligible. Thus, we do not consider correlations between the two ions' internal dynamics that would lead to cooperative effects such as superradiance. We rather calculate the cooling effect that each of the two ions individually has on the common motion. This effect is the same for both ions, since the foci of the lasers are wide compared with the distance of the ions (the waist of the Gaussian beams being  $w \approx 10 r_0$ ), and therefore the laser intensities, and consequently laser cooling do not depend on the ions' positions.

We shall now give a short recap of the theory presented in Ref. [12] and apply its results to the collective motion of two ions in the current experiment. We start from the density operator  $\varrho$  for the motional and internal degrees of freedom. The dynamics is described by the master equation

$$\frac{d}{dt}\varrho(t) = \frac{1}{i\hbar}[H, \varrho(t)] + \mathcal{L}\varrho(t) \quad , \quad (10)$$

where

$$\begin{aligned} \mathcal{L}\varrho = \sum_{j=1,2} \sum_l \gamma_l \left( 2\sigma_{l,j}^- \int_{-1}^1 d\zeta W_l(\zeta) e^{-ik_l r_j \zeta} \varrho e^{ik_l r_j \zeta} \sigma_{l,j}^+ \right. \\ \left. - \sigma_{l,j}^+ \sigma_{l,j}^- \varrho - \varrho \sigma_{l,j}^+ \sigma_{l,j}^- \right) \end{aligned} \quad (11)$$

is the Liouvillian allowing for spontaneous emission. It has the usual Lindblad form [14], where dissipation acts on the internal (via  $\sigma^\pm$ ) and on the motional (via  $e^{\pm i\mathbf{k} \cdot \mathbf{r}}$ ) degrees of freedom. The index  $j$  labels the two ions, and

the index  $l$  runs over all atomic transitions involved.  $2\gamma_l$  is the spontaneous emission rate, and  $\sigma_l^\pm$  are the corresponding transition operators.  $W_l(\zeta)$  is the angular distribution of spontaneous emission for this transition. The Hamiltonian is given by

$$H = \frac{\mathbf{P}^2}{2M} + V(\mathbf{R}) + \frac{\mathbf{p}^2}{2\mu} + V(\mathbf{r}) + \sum_{j=1,2} H_{\text{in},j} + V_{\text{Dip},j} \quad (12)$$

$H_{\text{in},j}$  is the Hamiltonian for the internal levels of the  $j$ -th ion. The ion's dipole interaction with the laser light can be written as

$$V_{\text{Dip},j} = \sum_l \hbar\Omega_l e^{i\mathbf{k}_l \cdot \mathbf{r}_j} \sigma_{l,j}^+ + \text{H.c.} \quad , \quad (13)$$

where  $\Omega_l$  is the Rabi frequency of the light driving the transition  $l$ . Summing over both ions, and rewriting the dipole interaction in terms of center-of-mass and relative coordinates [(Eq. 3)], gives

$$V_{\text{Dip}} = \sum_l \hbar\Omega_l e^{i\mathbf{k}_l \cdot \mathbf{R}} \left( e^{-\frac{i}{2}\mathbf{k}_l \cdot \mathbf{r}} \sigma_{l,1}^+ + e^{\frac{i}{2}\mathbf{k}_l \cdot \mathbf{r}} \sigma_{l,2}^+ \right) + \text{H.c.} \quad (14)$$

Note that the center-of-mass and relative motions are coupled via the interaction with the laser light. However, in the Lamb-Dicke limit this coupling can be neglected, as  $\langle \mathbf{k}_l \cdot \mathbf{R} \rangle$ , and  $\langle \mathbf{k}_l \cdot \tilde{\mathbf{r}} \rangle$  are small and the potential can be expanded. This expansion is characterized by the Lamb-Dicke parameters

$$\eta_{l,q} = \mathbf{k}_l \cdot \mathbf{e}_q \sqrt{\hbar/2m\omega_q} \quad (15)$$

for the center-of-mass modes and  $\tilde{\eta}_{l,q} = \mathbf{k}_l \cdot \mathbf{e}_q \sqrt{\hbar/2m\tilde{\omega}_q}$  for the normal modes of the relative motion. In the experiment, all LDPs are much smaller than unity, see Table I. Now, we rewrite the coordinates in terms of the lowering and raising operators of the corresponding vibrational eigenmodes

$$R_q = \sqrt{\frac{\hbar}{2M\omega_q}} (a_q^\dagger + a_q) \quad , \quad \tilde{r}_q = \sqrt{\frac{\hbar}{2\mu\tilde{\omega}_q}} (\tilde{a}_q^\dagger + \tilde{a}_q) \quad (16)$$

Since the expansion is around the potential minimum, there is a constant phase factor  $e^{\pm \frac{i}{2}\mathbf{k}_l \cdot \mathbf{r}_0}$ , that is incorporated in the atomic transition operators  $\sigma_{l,j}^\pm$ . Now, keeping only terms up to first order in (any) Lamb-Dicke parameter yields

$$\begin{aligned} V_{\text{dip}} = \sum_{j=1,2} \sum_l \hbar\Omega_l \sigma_{l,j}^x - \frac{1}{\sqrt{2}} \sum_q \hbar\Omega_l \eta_{l,q} (a_q^\dagger + a_q) \sigma_{l,j}^y \\ - \frac{(-1)^j}{\sqrt{2}} \sum_q \hbar\Omega_l \tilde{\eta}_{l,q} (\tilde{a}_q^\dagger + \tilde{a}_q) \sigma_{l,j}^y \quad , \end{aligned} \quad (17)$$

where  $\sigma^x = \sigma^+ + \sigma^-$  and  $\sigma^y = (\sigma^+ - \sigma^-)/i$  have been used. The first term of Eq. (17) describes the driving of the internal dynamics by the interaction with the laser light. Since it is of zeroth order in any LDP it does not contain the mechanical effect of light, i.e. no laser cooling or heating. The second and third term of Eq. (17) (first order in a LDP) couple the internal dynamics to the center-of-mass and relative motions, respectively. The ion-dependent sign in the third line of Eq. (17) arises from the opposite impact of the two ions' recoil on the relative motion. Since the vibrational modes decouple in the Lamb-Dicke limit, we can restrict ourselves to a 1D description. Therefore, the index  $q$  characterizing the specific mode is omitted in what follows.

Now, the fast internal dynamics of the ions is adiabatically eliminated and one obtains a master equation for the external degrees of freedom. This procedure finally leads to the well known time evolution of the mean phonon number [15]

$$\frac{d}{dt}\langle n \rangle = -(A_- - A_+)\langle n \rangle + A_+ \quad , \quad (18)$$

with the cooling rate

$$W = A_- - A_+ \quad (19)$$

and (if the cooling rate is positive) the mean motional energy

$$E_{\text{Ex}} = \hbar\omega \frac{A_+}{A_- - A_+} \quad . \quad (20)$$

The transition rates  $A_{\pm}$  are given by

$$A_{\pm} = 2(\text{Re}S(\mp\omega) + D) \quad . \quad (21)$$

The first constituent is the fluctuation spectrum of the electronic dipole coupling

$$S(\omega) = \sum_{l,l'} \Omega_l \Omega_{l'} \eta_l \eta_{l'} \int_0^{\infty} dt e^{i\omega t} \langle \sigma_l^y(t) \sigma_{l'}^y(0) \rangle, \quad (22)$$

where  $\omega$  is the vibrational frequency of the considered mode. The expectation value is to be taken in the steady state of the internal dynamics that in turn is calculated from the master equation

$$\frac{d}{dt} \varrho_{\text{in}}(t) = \frac{1}{i\hbar} \left[ H_{\text{in}} + \sum_l \hbar \Omega_l \sigma_l^x, \varrho_{\text{in}}(t) \right] + \mathcal{L}_0 \varrho_{\text{in}}(t) \quad , \quad (23)$$

derived from Eq. (10), by using adiabatic elimination, and keeping only the zeroth order in any LDP. Here,

$$\mathcal{L}_0 \varrho_{\text{in}} = \sum_l \gamma_l (2\sigma_l^- \varrho_{\text{in}} \sigma_l^+ - \sigma_l^+ \sigma_l^- \varrho_{\text{in}} - \varrho_{\text{in}} \sigma_l^+ \sigma_l^-) \quad (24)$$

describes the spontaneous emission in zeroth order. Via the driving by laser light, the steady state depends on

the parameters (intensity, detuning, polarization) of the light field.

The second contribution to the transition rates originates from the spontaneously emitted photons as described by the Liouvillian  $\mathcal{L}$ . So far, spontaneous emission has only been considered up to the zeroth order in the LDP. The second order term is readily calculated and leads to the additional transition rate

$$D = \sum_l \gamma_l \frac{\alpha_l}{(\mathbf{k}_l \cdot \mathbf{e}_q)^2} \eta_l^2 \langle \sigma_l^+ \sigma_l^- \rangle \quad (25)$$

both from  $|n\rangle$  to  $|n+1\rangle$  and vice versa. Here, the geometrical factor  $(\mathbf{k}_l \cdot \mathbf{e}_q)^2$  in the LDP (eq. 15) is replaced by  $\alpha_l = \int_{-1}^1 d\zeta W_l(\zeta) \zeta^2$  that accounts for the angular distribution of the light emission.

### III. EXPERIMENTAL OBSERVATION

The two Ba<sup>+</sup>-ions are confined in a 1-mm-diameter Paul trap and irradiated by laser light at 493 nm for excitation of resonance scattering on the  $^2\text{S}_{1/2}$ - $^2\text{P}_{1/2}$  transition. This laser is detuned slightly below resonance for cooling the ions. The fluorescence signal is recorded by photon counting. A second laser at 650 nm prevents optical pumping into the  $^2\text{D}_{3/2}$  level. A static magnetic field defines the quantization direction and lifts the degeneracy of the magnetic sublevels. Its direction is at 45 degrees with respect to the plane defined by the ring electrode. The directions of propagation and the polarizations of both light beams are set perpendicular to the magnetic field. The power levels of the light fields are stabilized by electro-optic modulators. Precise detuning of the 650-nm laser is accomplished using a double-pass acousto-optic modulator. So far, the setup has been described elsewhere [16]. In addition the fluorescent light is monitored by a spatially resolving photo multiplier revealing the position of the ions in the trap.

The ions are dynamically trapped by superimposed electric dc and rf-fields [17] and represent particles inside a nearly spheroidal harmonic (quasi)potential. In order to determine the geometry of this (quasi)potential oscillations of a single trapped ion are excited by applying an additional rf field. Three sharp resonances are found at the frequencies given in Table I, i.e. macroscopic motion of the ion in the  $x$ ,  $y$  and/or  $z$  direction of the trap is observed. The  $x$ -direction, within the radial plane, is found at approximately 45 degrees to the polarization of the lasers. While the nondegeneracy of  $\omega_z$  is obvious, the asymmetry of  $\omega_x$  and  $\omega_y$  originates from a slight asymmetry of the ring electrode. The distance of the two ions in the potential minima, as calculated from Eq. (6) using the actual values of  $\mu$  and  $\omega_q$  is  $r_0 = 3.70 \mu\text{m}$  and agrees very well with the experimental value  $3.65 \mu\text{m}$  obtained from the spatially resolved measurement.

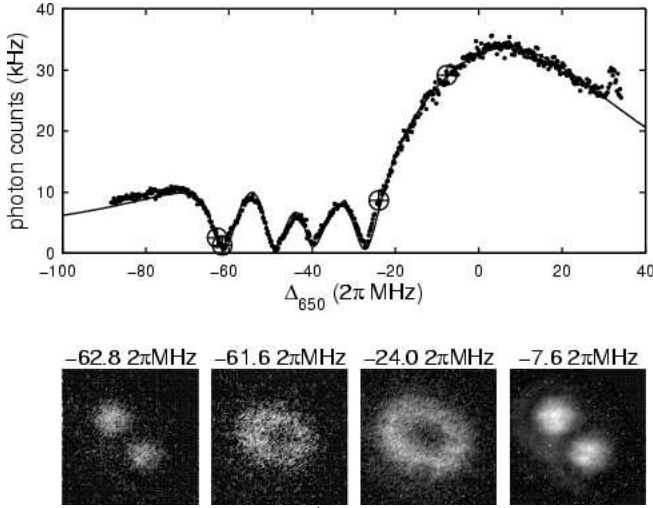


FIG. 2. Two trapped  $\text{Ba}^+$  ions show different motional states depending on laser parameters. Top: fluorescence of two trapped ions as a function of laser detuning, collected in 0.1s. Bottom: spatial distribution of the two ions at the detunings indicated above.

Keeping all other parameters constant, the frequency of the 650-nm laser is scanned across the  $^2\text{D}_{3/2}\text{-}^2\text{P}_{1/2}$  line. The intensity of the scattered light vs detuning of the 650-nm light,  $\Delta_{650} = \omega_{650} - \omega_{\text{P}\leftrightarrow\text{D}}$ , is shown in the upper part of Fig. 2, where  $\omega_{650}$  is the laser frequency and  $\omega_{\text{P}\leftrightarrow\text{D}}$  is the atomic transition frequency. The structure of dark resonances is well known from the fluorescence of a single ion [18] and corresponds to four dark states, i.e. coherent superpositions of magnetic substates of the  $^2\text{S}_{1/2}$  and  $^2\text{D}_{3/2}$  levels, respectively. From a fit of this excitation spectrum with eight-level optical Bloch equations, accounting for the Zeeman substructure, we obtain the Rabi frequencies of both lasers, the detuning  $\Delta_{493} = \omega_{493} - \omega_{\text{S}\leftrightarrow\text{P}}$  of the 493 nm laser as well as the strength of the magnetic field. This is a standard procedure in our  $\text{Ba}^+$  experiments. The parameters obtained from the spectrum shown in Fig. 2 are  $\Omega_{650} = 59.0 \times 2\pi$  MHz,  $\Omega_{493} = 46.2 \times 2\pi$  MHz,  $\Delta_{493} = -44.3 \times 2\pi$  MHz and  $B/\hbar\mu_B = 7.7 \times 2\pi$  MHz, where  $\mu_B$  is the Bohr magneton.

Additional information is derived from monitoring the motion of the two ions. Depending on the detuning of the 650-nm laser, different motional states are observed. Whereas the ions appear at fixed positions if the red laser is tuned below the lowest or well above the highest dark resonance, they form a ring-shaped distribution in the  $(x, y)$  plane with certain intermediate detunings.

The lower part of Fig. 2 shows the motional state at four different detunings, corresponding to the crosshairs in the spectrum. Note the clear distinction of the localized state at  $\Delta_{650} = -62.8 \times 2\pi$  MHz from the non-localized state only  $2.6 \times 2\pi$  MHz away: Phase transitions between the two observed motional states appear at very definite laser frequencies.

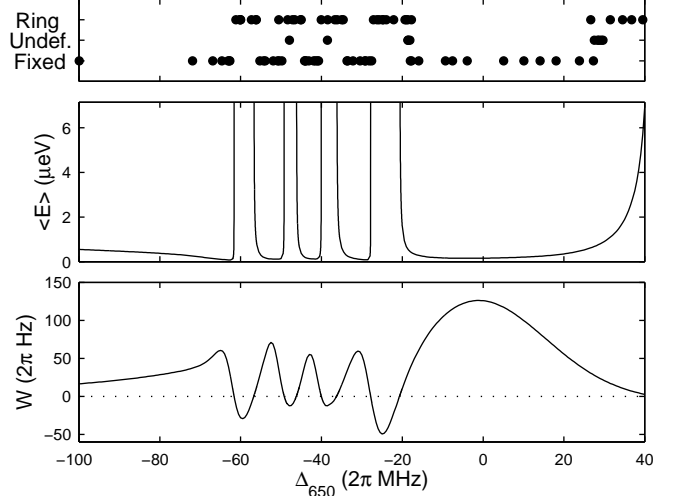


FIG. 3. Top: observed motional states for different detunings of the 650-nm light. The dots correspond to individual observations. Middle: mean motional energy in the  $\tilde{y}$ -mode calculated from theory. Bottom: cooling rate for the  $\tilde{y}$ -mode calculated from theory.

Obviously, the motional state of the ions depends on the ion temperature set by the laser cooling. In Fig. 3, the motional states observed at different detunings are shown together with the motional energies and cooling rates calculated from theory. The different motional states appear in distinct regions of detuning: The ions are observed in the fixed position for the detuning  $\Delta_{650}$  below  $-61 \times 2\pi$  MHz. At this limiting value a sharp phase transition occurs, and the ions form a ring when  $-61 \times 2\pi$  MHz  $< \Delta_{650} < -56 \times 2\pi$  MHz. At the upper boundary, they are cooled again to the fixed-position state. Such a “hot” region appears with each dark resonance. At some values of the detuning, e.g. at  $\Delta_{650} = -19 \times 2\pi$  MHz, the motion fluctuated between the fixed and the ring-shaped state, thus remaining indefinite.

The motional energy has been calculated from the model presented in the preceding section, using the experimental values for the  $\tilde{y}$ -mode. This energy should be compared with the height of the potential barrier [(Eq. 7)], which for the given data is  $\Delta V_y = 7.15 \mu\text{eV}$ . Wherever the predicted temperature varies steeply upon detuning, a sharp transition is observed. This is the case, when the corresponding cooling rate changes from positive to negative, i.e. when the lasers actually heat the ion. Laser heating appears at *negative* detunings of both lasers when Raman transitions dominate the interaction. In the vicinity of the dark resonances, the internal state consists of a coherent superposition of the  $\text{S}_{1/2}$  and the  $\text{D}_{3/2}$  states, forming an effective two level system. Now, with both detunings being negative, and  $\Delta_{650} > \Delta_{493} + \Delta_{\text{zee}}$ , the effective detuning of this Raman transition is positive, and causes heating of the motion. Here,  $\Delta_{\text{zee}}$  is the difference in Zeeman shifts of the involved sublevels that

defines the resonance condition of the considered dark state.

Note that the transition to the ring state, at positive detunings from the Raman resonances, appears where the expected energy is still considerable lower than the potential barrier. However, this does not contradict the model, which assumes the ions close to the potential minima. As soon as they are smeared out over a region of considerable size, the harmonic approximation around the minimum no longer holds. The cooling gets less effective for the broadened velocity distribution. This happens when the thermal energy is substantially lower than  $\Delta V_y$ . Still, the observed phase transitions agree very well with the results of the model.

At low speed of scanning, for example,  $d\Delta_{650}/dt \approx 1 \times 2\pi$  MHz/s, we observed hysteresis effects: The motional state upon up-tuning the laser frequency differed from the state observed upon down-tuning. However, this effect vanished when the scanning rate was decreased. Scans at a very low speed ( $d\Delta_{650}/dt \lesssim 0.1 \times 2\pi$  MHz/s) showed that the motional state solely depends on the laser parameters. Therefore, a steady state exists, which is approached in a finite motional relaxation time.

The final temperature is, in principle, not only set by the laser cooling, but it is subject to additional heating mechanisms, such as fluctuations in the trapping electric field. However, the calculated transition rates  $A_{\pm} \approx 10^5 \dots 10^6$  s $^{-1}$  equal the number of scattered phonons per unit time, and thus exceed the rate of parasitic heating ( $\approx 10 \dots 10^4$  s $^{-1}$ ) observed in ion trap experiments [19]. Therefore, this additional heating can be neglected as long as the ions are kept laser-cooled.

#### IV. OPTIMIZATION OF LASER COOLING

The discussed model is now employed to numerically investigate the influence of various parameters on the laser cooling, and to find optimized conditions for effective and robust cooling. We concentrate on the  $\tilde{x}$  (stretch)mode, since it is less affected by perturbations from stray fields of the trap [20] and therefore is suitable for serving as a bus mode between the ions. A promising candidate for implementing qubits in trapped Ba $^{+}$  is the  $S_{1/2}$ - $D_{5/2}$  (1762 nm) transition [21]. The LDP corresponding to this infrared transition is smaller than those of other transitions (see Table I), and the Sørensen-Mølmer criterion  $\eta^2 \langle n \rangle + 1 \ll 1$  yields the condition  $\langle n \rangle \ll 10^4$  that is easily fulfilled in practice. In fact, a mean phonon number  $\langle n \rangle < 1$  can be reached: This is shown in the middle part of Fig. 4, where  $\langle n \rangle$  is plotted vs the detuning of the 650-nm light. The lowest vibrational excitation was found by randomly searching the 4D parameter space for the lowest achievable  $\langle n \rangle$ . Then, three laser parameters were kept constant, while the red-laser detuning was varied, in order to generate the graph. The minimal temperature is achieved around  $\Delta_{650} \approx 6 \times 2\pi$

MHz. Note that the lowest value  $\langle n \rangle = 0.9$  indicated by the vertical dotted line does not match a particularly large cooling rate, as is shown in the lower part of Fig. 4. Looking at the expected fluorescence signal (upper part of the Figure), we note that the optimum detuning is on the red side of the dark resonance at  $\Delta_{650} = 4.9 \times 2\pi$  MHz, as is expected for Raman cooling. The dark resonance is power broadened by the high intensity at 650 nm. On the other hand, we find low temperatures only for low intensity of the 493-nm light. This fact indicates that scattering of the blue light is the dominant heating mechanism. We do not claim to have found the absolute minimum of achievable temperature: Other sets of laser parameters may yield similarly low temperatures, and also the applied magnetic field to some degree influences the achievable temperature.

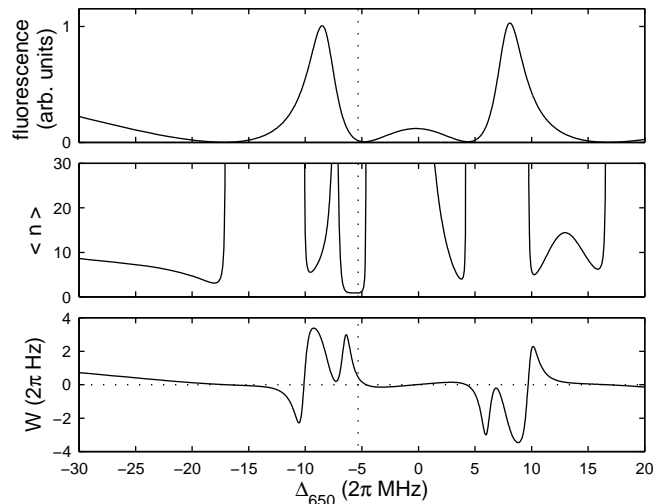


FIG. 4. Fluorescence, mean number of vibrational quanta in the  $\tilde{x}$ -mode, and cooling rate vs laser detuning. The vertical dotted line indicates the minimal  $\langle n \rangle$ , laser parameters:  $\Omega_{650} = 89.6 \times 2\pi$  MHz,  $\Omega_{493} = 2.1 \times 2\pi$  MHz,  $\Delta_{493} = -0.21 \times 2\pi$  MHz. Other parameters as in Sec. III

We have restricted the parameter search to the range of negative detuning. Even lower energies may be reached with both lasers detuned to the blue side of the atomic resonance and the parameters adjusted to yield so-called electromagnetically induced transparency cooling [22]. Here, the dynamic Stark contribution to the nonlinear susceptibility dominates the interaction of ions and light [23]. However, Doppler precooling is still necessary and the lasers must either be switched from negative to positive detuning, or else additional light sources are required. Moreover, the intensities of the lasers must be precisely controlled, since for this type of cooling to work, the dynamic Stark shift should match the vibrational frequency particularly well. However, cooling mechanisms are desirable, that are more robust against variations of

intensity and detuning of the laser light, and thus are easier to implement experimentally.

The robustness of the cooling is affected by the sharp boundaries between parameter regimes of very low and high temperature, because in these regions any drift of the lasers' frequencies may cause drastic deterioration of the cooling. In order to find "safe" parameters we repeated the search, incorporating a tentative drift in the following way: For a given point in the  $(\Delta_{493}, \Delta_{650})$  parameter plane,  $\langle n \rangle$  was calculated at this point and at eight additional points, where one or both of the detunings differ by  $\pm 1 \times 2\pi$  MHz, and then averaged over the  $\langle n \rangle$  values at all nine points. The best robust parameters found differ from the ones used to calculate Fig. 4 and the achievable ion temperature is not as low as in the ideal situation, but one still finds  $\langle n \rangle = 3.3$ . The result is shown in Fig. 5, where the mean phonon number is shown as a function of  $\Delta_{650}$  (solid line). The dotted line shows, for comparison, the vibrational excitation that is achieved with the same parameters, when the averaging over nine points is *not* carried out. The regions of safe cooling are narrower, since detuning close to a "boundary" between cooling and heating is penalized. It seems not advisable to use a rather narrow region of cooling (as, for example, close to  $\Delta_{650} \approx -7 \times 2\pi$  MHz), because spurious laser drift might easily impose unexpected heating. However, some regions [e.g.  $\Delta_{650} \approx (-22 \text{ to } -17) \times 2\pi$  MHz and  $\Delta_{650} \approx (-5 \text{ to } 5) \times 2\pi$  MHz] are broad enough to allow for some laser drift with satisfactory cooling.

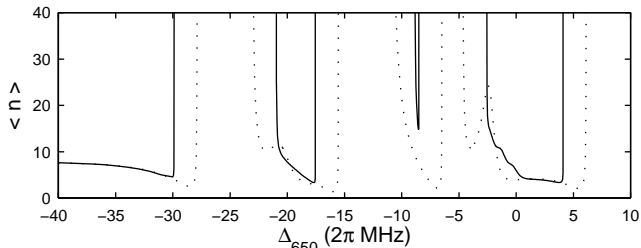


FIG. 5. Mean number of vibrational quanta for fixed laser parameters (dotted) and averaged over nine combinations of both detunings (see text) (solid). Laser parameters:  $\Omega_{650} = 59.5 \times 2\pi$  MHz,  $\Omega_{493} = 3.8 \times 2\pi$  MHz,  $\Delta_{493} = -10.9 \times 2\pi$  MHz. Other parameters as in Sec. III

## V. CONCLUSION

We have observed the effect of laser cooling and heating on the collective motion of two trapped  $\text{Ba}^+$  ions by monitoring the macroscopic motional states of the ions. These states indicate the vibrational excitation, or temperature of the ions. In this way, Raman heating is demonstrated that dominates on the blue side of the dark resonances (i.e.  $\Delta_{650} > \Delta_{493} + \Delta_{Zee}$ ).

The observed phase transitions are a remarkable macroscopic manifestation of dark states, i.e. of the coherent quantum superposition of atomic levels. Raman

cooling on the red side of the dark resonance is implied, though it is not directly observed with this method, since no macroscopic change of the motional state shows up.

The good agreement of the calculated excitation with the experimental observations shows that the outlined theory describes well the laser cooling of the collective motion of the ions. The predicted cooling rates much exceed spurious heating rates of the vibrational motion, for example, from fluctuations of the trapping electric field. Thus, such heating is negligible as long as the cooling light is on.

The model comes with no free parameters; however, it is applicable only if the ions are localized near their potential wells. Nevertheless, this is not a strong restriction since this regime is supposed to be used in any experiment implementing conditional quantum dynamics. This allows us to identify parameter regimes that imply effective and robust laser cooling. We find that the collective motion can become cooled close to the ground state, if the dark resonances are not much broadened by laser power or fluctuations. But even when fluctuations in laser parameters are allowed for, low levels of temperature emerge that are suitable for quantum information processing using the scheme for conditional quantum dynamics suggested by Sørensen and Mølmer [2]. We note that the level scheme of  $\text{Ba}^+$  has the same structure as, for example,  $\text{Ca}^+$  [24], a type of ion often suggested, and the results obtained here are applicable, with appropriate modifications, to the cooling of these ions, too.

- 
- [1] J. I. Cirac and P. Zoller, Phys. Rev. Lett. **74**, 4091 (1995).
  - [2] A. Sørensen and K. Mølmer, Phys. Rev. Lett. **82**, 1971 (1999).
  - [3] S. Stenholm, Review of Modern Physics **58**, 699 (1986).
  - [4] B. W. Shore and P. L. Knight, J. Mod. Opt. **40**, 1195 (1993).
  - [5] D. Jonathan, M. B. Plenio, and P. L. Knight, Phys. Rev. A **62**, 042307 (2000).
  - [6] Th. Sauter, H. Gilhaus, W. Neuhauser, R. Blatt, and P. E. Toschek, Europhys. Lett. **7**, 317 (1988).
  - [7] R. Blümel, J. M. Chen, E. Peik, W. Quint, W. Schleich, Y. R. Shen, and H. Walter, Nature **334**, 309 (1988).
  - [8] Th. Sauter, H. Gilhaus, I. Siemers, R. Blatt, W. Neuhauser, and P. E. Toschek, Z. Phys. D **10**, 153 (1988).
  - [9] W. Neuhauser, M. Hohenstatt, P. E. Toschek, and H. G. Dehmelt, Phys. Rev. Lett. **41**, 233 (1978).
  - [10] C. Monroe, D. M. Meekhof, B. E. King, S. R. Jefferts, W. M. Itano, D. J. Wineland, and P. Gould Phys. Rev. Lett. **75**, 4011 (1995).
  - [11] H. Gilhaus, T. Sauter, W. Neuhauser, R. Blatt, and P. E. Toschek Opt. Comm. **69**, 25 (1988).
  - [12] D. Reiß, A. Lindner, and R. Blatt, Phys. Rev. A **54**, 5133 (1996).

- [13] A. Beige, and G. C. Hegerfeldt, *Phys. Rev. A* **59**, 2385 (1999)
- [14] G. Lindblad, *Commun. math. Phys.* **48**, 119 (1976).
- [15] M. Lindberg, J. Javanainen, *J. Opt. Soc. Am. B* **3**, 1008 (1986).
- [16] M. Schubert, I. Siemers, R. Blatt, W. Neuhauser, and P. E. Toschek, *Phys. Rev. A* **52**, 2994 (1995).
- [17] W. Neuhauser, M. Hohenstatt, P. E. Toschek, and H. G. Dehmelt, *Phys. Rev. A* **22**, 1137 (1980).
- [18] Y. Stalgies, I. Siemers, B. Appasamy, and P. E. Toschek, *J. Opt. Soc. Am. B* **15**, 2505 (1998).
- [19] H. Rohde, S. T. Gulde, C. F. Roos, P. A. Barton, D. Leibfried, J. Eschner, F. Schmidt-Kaler, and R. Blatt, [quant-ph/0009031](https://arxiv.org/abs/quant-ph/0009031) (unpublished).
- [20] B. E. King, C. S. Wood, C. J. Myatt, Q. A. Turchette, D. Leibfried, W. M. Itano, C. Monroe, and D. J. Wineland, *Phys. Rev. Lett.* **81**, 1525 (1998).
- [21] B. Appasamy, Y. Stalgies, P. E. Toschek, *Phys. Rev. Lett.* **80**, 2805 (1998).
- [22] G. Morigi, J. Eschner, C. H. Keitel, *Phys. Rev. Lett.* **85**, 4458 (2000); C. F. Roos, D. Leibfried, A. Mundt, F. Schmidt-Kaler, J. Eschner, and R. Blatt, *Phys. Rev. Lett.* **85**, 5547 (2000).
- [23] Th. Hänsch, P. E. Toschek, *Z. Physik* **236**, 213 (1970).
- [24] For example, A. Steane, *Appl. Phys. B* **64**, 623 (1997).